

## Electrochemistry in Near-Critical and Supercritical Fluids. 9. Improved Apparatus for Water Systems (23–385 °C). The Oxidation of Hydroquinone and Iodide

Chong-yang Liu, Shelly R. Snyder, and Allen J. Bard\*

Department of Chemistry and Biochemistry, The University of Texas at Austin, Austin, Texas 78712

Received: September 10, 1996<sup>⊗</sup>

The apparatus for electrochemical measurements in high-temperature water has been improved by replacing the alumina tube reactor with an oxidized titanium tube, producing a more rugged reactor. All metal fittings were replaced by titanium ones, decreasing corrosion problems. The working electrodes are Pt disks (radius, 14  $\mu\text{m}$ ) fabricated by sealing Pt–Ir wires in a high PbO-containing glass. This glass has the advantage over borosilicate glass in showing lower conductivity at temperatures above 230 °C, better corrosion resistance, and a coefficient of thermal expansion well-matched to Pt. Well-defined steady-state cyclic voltammograms for the oxidation of iodide ion and hydroquinone were obtained in (initially 23 °C) 0.2 M NaHSO<sub>4</sub> solutions over a temperature range 23–385 °C. Diffusion coefficients (*D*) were determined from the limiting currents. The experimental *D* values were in excellent agreement with those calculated from the Stokes–Einstein equation and viscosity values for water at the relevant temperatures and pressures.

### Introduction

Near-critical and supercritical water is of interest in both fundamental studies and practical applications. The thermodynamic and chemical properties of water change substantially with temperature and pressure.<sup>1</sup> The density, dielectric constant,  $\epsilon$ , and viscosity all show large decreases as the temperature rises to the critical point ( $T_c = 374$  °C,  $P_c = 221$  bar).<sup>2–6</sup> For example,  $\epsilon$  decreases from 80 at room temperature to about 5 at the critical point. Thus, many nonpolar organic compounds will dissolve in near-critical water. Near the critical point, small changes in pressure and temperature result in large changes in the properties of water. The low viscosity and high temperatures also promote reaction kinetics. Thus, supercritical water containing oxygen is capable of complete oxidation of many pollutants<sup>7</sup> and is potentially useful in the destruction of wastes, chemical warfare agents, and explosives. The development of electrochemical sensors and a better understanding of electron-transfer reactions in high-temperature water would also be of interest in the electric power and manufacturing industries.<sup>8</sup>

Electrochemical measurements in high-temperature water are challenging. Aqueous solutions under these conditions are very corrosive and can attack most metals and dissolve quartz and Pyrex glass, leading to equipment failure and solution contamination. Thus, a major effort of past work in our group<sup>9–12</sup> has been in the design of cells and electrodes that allow precise measurements under these conditions. One of the difficulties in earlier experiments<sup>10–12</sup> was in the use of an alumina tube as the electrochemical cell. Although alumina has the desired properties of chemical inertness to hot water and a high volume resistivity (reducing stray electric fields within the cell during electrochemical measurements), it is somewhat brittle and has a tendency to break under high pressure and temperature conditions. Experiments frequently had to be terminated during a heating cycle when the alumina tube cracked (and sometimes exploded). To circumvent this problem, alternative materials with a higher mechanical strength were investigated. The basic design of the cell, which has an exchangeable central heated reactor, allows for the incorporation of different reactor materials and for the removal and inspection of the central heated tube for signs of fatigue and wear. Since the cell volume is only

about 2 mL, failures and leaks are not dangerous. All measurements in this work were carried out in an improved electrochemical cell based on an oxidized titanium tube that showed excellent mechanical and chemical stability. All other parts of the apparatus connecting to the cell, originally of 316 stainless steel and Hastelloy, were also changed to titanium, eliminating the contamination from metal corrosion.

Another important improvement was in electrode design. Most of the previous cells<sup>9,10</sup> used macroscopic electrodes. At the current levels characteristic of such electrodes the resistive (*iR*) drops were significant, especially at high temperatures where solution resistance increases, and this limited the accuracy of the measurements. One attempt was made to use an ultramicroelectrode of Pt sealed in Pyrex.<sup>11</sup> However, the expected sigmoidal voltammograms, characteristic of steady-state conditions at an ultramicroelectrode, were not observed, and the electrode area appeared much larger at the high temperatures. We now recognize that a Pyrex electrode suffers from corrosion and current leakage through the glass walls at high temperature. The mismatch between the thermal expansion coefficients of Pt and Pyrex also led to electrode leaks when the electrode was subjected to high temperatures. Another goal in this study was the fabrication of ultramicroelectrodes by sealing Pt in a chemically inert glass with a high electrical resistance at high temperatures and a thermal expansion coefficient close to that of Pt.

### Experimental Section

**Electrochemical Cell.** The high-pressure and high-temperature electrochemical cell used in this study was of the same general configuration employed in previous experiments.<sup>10,11</sup> Replacing the alumina tube to improve the mechanical stability with 316 stainless steel, Inconel 625, Hastelloy C-276, or monel proved unsatisfactory because they all showed the presence of corrosion products during trials. The outlet stream was routinely monitored for the presence of ferrous iron spectrophotometrically after addition of *o*-phenanthroline. Successful modification was achieved by the replacement of the alumina tube with one of oxidized titanium, as shown schematically in Figure 1. The major advantages of a Ti tube are its greater structural integrity and chemical inertness. Ti tubes were either anodically oxidized in H<sub>2</sub>SO<sub>4</sub> or thermally oxidized at 600 °C for ~5 h in an oven.<sup>13</sup>

<sup>⊗</sup> Abstract published in *Advance ACS Abstracts*, January 15, 1997.

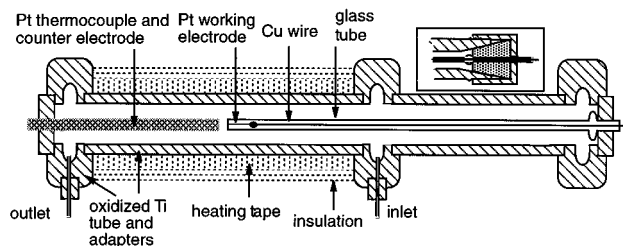


**Figure 1.** Schematic diagram of high-temperature, high-pressure electrochemical cell. The inset shows the configuration of a joint with glass tube, ferrule, cell tube, and nut. All joints were essentially the same in structure. In the actual cell, additional Ti tubes were used to bridge the inlet and outlet tubings to the cell in the hot zone so that the PEEK tubings were always in a relatively cool zone similar to the joint holding the working electrode.

Prior to anodization, the tubes were degassed in trichloroethane and subsequently rinsed with distilled water. Oxidized tubes appeared grayish-blue in color, presumably because of the incorporation of hydrated Ti species in the form of  $\text{Ti}(\text{OH})_3$  within the oxide film. The oxide layer on Ti was electrically insulating over a much larger temperature range than that of 316 stainless steel and is also chemically inert. Ti tubes could be used, without repassivation, for more than 20 experiments without mechanical failure or loss of performance. Based on the exceptional performance of Ti as a material in our supercritical water apparatus, all 316 stainless steel and Hastelloy parts in the original design were replaced with Ti parts. The central section of the cell consisted of a 6.35 mm (1/4 in.) o.d. Ti (99.6%) tube with 0.89 mm diameter wall thickness and a length of 10 cm (Goodfellow). The tube contained solution under high pressure and was the only section of the cell that was heated. Heating was accomplished by wrapping the tube in a flexible electric heating tape (Omegalux Model STH051-020) around which asbestos insulation and Zertex heating cloth was wrapped. The central tube was fitted to the Ti end blocks via Swagelock Ti fittings and ferrules (1/4 in.).

Inlet and outlet tubing from the cell body was 1/16 in. PEEK (polyetheretherketone) tubing. This composite has a higher continuous operating temperature than Teflon (400 vs 250 °C, respectively), but it is still compressible and maintains pressures up to 6000 psi. PEEK tubing also allowed better electrical isolation of the cell from the electrical components of the apparatus than previously possible with stainless steel tubing and is chemically inert and corrosion-free. The PEEK tubing was fitted to 1/4 in. Swagelock fittings using 60% Vespel/40% graphite reducing ferrules. The solution was introduced into the cell with a metal-free dual-piston HPLC pump without concern for the introduction of corrosion products from the pump. The pressure was monitored with a pressure gauge (Sensotec) inserted between the outlet of the cell and valve to the outlet reservoir.

A platinum-sheathed R-type thermocouple (Omega) was inserted into one of the horizontal entry ports on the Ti end block and was maintained in place using Vespel/40% graphite reducing ferrules secured with a 1/4 in. Ti Swagelock nut. The thermocouple probe was connected to a programmable home-built temperature controller (Omega Model CN76000). The controller could be programmed to ramp linearly over a specified time interval and was capable of controlling the temperature of the cell to within 1 °C of the desired value. Experiments where the thermocouple was cemented to the outside of the Ti tube gave erroneous cell temperature measurements. Plots of the cell temperature inside vs outside the tube were linear over the temperature range used in supercritical water studies. However,

the temperature differences between the outside and inside of the tube, e.g., at 300 °C, were greater than 40 °C.

The working electrode consisted of a platinum wire enclosed in a glass capillary tube, which ran directly through the hole in a Vespel/graphite ferrule to the external (atmospheric) side of the cell and was secured with a 1/4 in. Swagelock Ti compression fitting. This modification eliminated the glass-to-metal Kovar seal in the earlier design, which was the point of breakage and a source of corrosion products. Because the glass tube cannot be overtightened without breaking, a perfectly sealed electrochemical cell at room temperature could leak to a certain degree at higher temperatures simply because of the differences in thermal expansion coefficients of the glass tube, Vespel/graphite ferrule, and titanium nut. Therefore, the working electrode was fixed to the cell at a relatively cool zone as shown in Figure 1. However, it was sometimes still necessary to tighten the nut a little bit at high temperatures (>285 °C) to ensure a good seal. With this greatly improved electrochemical cell, breaking of the glass tube became the leading problem, although the use of a new ferrule for each experiment minimized this.

**Electrode Fabrication.** All experiments were carried out with ultramicroelectrodes made with a 25  $\mu\text{m}$  diameter platinum wire in a glass capillary tube according to literature procedures.<sup>14</sup> Briefly, a 25  $\mu\text{m}$  diameter platinum wire (99.95%, AESAR division of Johnson Matthey) was sealed in an end of a Pyrex or Corning 8870 glass tube (o.d. = 2 mm, i.d. = 1 mm, length = 15 cm; GTI Corp.). The Pt wire and glass must be heated very slowly to avoid the trapping of air bubbles that could expand and break the glass at high temperatures. The Pt disk electrode was exposed by successive polishing using 50 nm alumina at the last step. During the polishing, the electrodes were periodically checked under an optical microscope to be sure that a mirror-smooth surface without scratches was obtained. A Cu wire was connected to the Pt electrode with silver epoxy. The platinum thermocouple served as the counter electrode, which was about 5 mm away from the working electrode. A silver or platinum wire quasi-reference electrode was available in the cell but was not used in present studies.

**Procedure.** Chemicals and reagents were used as received without further purification. Solutions were deionized water from a Millipore, Milli-Q reagent water system. All experiments were conducted in solutions that had been deaerated with helium or argon pre-deoxygenated by passing through an Oxy-trap (Alltech Associates, Inc.). The temperature and pressure in the cell were controlled separately. During measurements, the outlet valve was closed so that the solution was stationary at the electrode. During heating processes, however, the outlet valve might be opened briefly when necessary to release solution to maintain the desired pressure. Data were collected at each temperature and pressure setting after allowing about 3–5 min for the solution to reach equilibrium. The disk-shaped Pt electrodes used for studying the cyclic voltammetry of  $\text{I}^-/\text{I}_2$  and hydroquinone/benzoquinone in 0.2 M  $\text{NaHSO}_4$  supporting electrolyte solutions had diameters of 29 and 28  $\mu\text{m}$ , respectively, as measured with an Olympus microscope (Model BH2). Cyclic voltammograms were obtained with a BAS-100A electrochemical analyzer (Bioanalytical Systems, Lafayette, IN). All the results shown in this paper are raw data without compensation or processing.

## Results and Discussion

**Ultramicroelectrode Voltammetry.** An ultramicroelectrode (UME) was used in this study primarily to reduce the large  $iR$ -drop in the cell, especially above the critical temperature where the solution resistance is high. However, we found it difficult

to fabricate a UME that was stable and useful over the wide temperature range required in these studies (25–385 °C). In general, with electrodes of Pt sealed in Pyrex, cyclic voltammograms (CVs) obtained above 250 °C had a clearly anomalous shape. A substantial slope developed that signaled leakage of solution between the Pt and surrounding glass sheath. This happened even with electrodes that routinely produced well-behaved steady-state voltammograms at temperatures below 100 °C. Sometimes when the cell temperature was decreased back to ambient conditions from high temperature, the CVs greatly improved. After a number of experiments, three major problems with these UMEs were identified.

**Glass Corrosion.** When the cell temperature was above ~300 °C, the solution that was removed from the cell appeared milky and the Pyrex glass surface of the electrode taken from the cell appeared frosted and opaque. Since there was a thick passive layer of TiO<sub>2</sub> on the Ti electrochemical cell surface, it was possible that the TiO<sub>2</sub> layer might have come off the Ti surface at high temperature and be deposited on the glass surface. However, X-ray photoelectron spectroscopic studies of the Pyrex glass surface following a high-temperature operation (~350 °C) revealed only Si (2p, s<sub>2</sub>), B (1s), and O (1s and Auger) species without any evidence of Ti. Thus, the observed phenomena were caused by the extensive corrosion of the Pyrex glass at high temperature. This could severely damage the glass seal of the electrode, cause leakage, and lead to a distorted voltammogram.<sup>14,15</sup>

**Thermal Expansion.** The coefficient of linear expansion of Pt is  $9.1 \times 10^{-6}/^{\circ}\text{C}$ , about 3 times higher than that for Pyrex glass. At a temperature of 375 °C, for example, we estimate that the Pt wire sealed within the Pyrex glass would extend out beyond the glass surface by more than 40 μm, assuming that they were coplanar at room temperature. Since the diameter of the Pt wire was only about 25 μm, the disk-shaped UME would gradually evolve into a cylindrical electrode as the temperature increased, and this was observed under an optical microscope by heating an electrode contained on a hot stage up to 300 °C. Moreover, the seal between the Pt wire and the glass would be substantially damaged by the relative movement caused by the thermal expansion.

**Glass Conductivity (Current Leakage).** At room temperature, Pyrex glass is a very good insulator and is widely used for electrode fabrication. However, at higher temperatures, Pyrex shows appreciable conductivity, i.e., significant current leakage through the glass wall of the electrode. Since the surface area of the sealing glass (~8 cm<sup>2</sup>) is more than 10<sup>6</sup> times greater than the end electrode area, any conductivity increase in the glass has a strong influence on the electrochemical signal. To test the extent of current leakage through the Pyrex, electrodes were fabricated without grinding and polishing the glass end so that the Pt wires were totally sealed inside the Pyrex glass tube and not exposed at all to solution. The *i*-*V* curves (Figure 2A) were always linear, and the slopes were taken as the conductance of the Pyrex glass under study. Figure 2B shows the measured conductance as a function of temperature. Under a bias of 1 V, the leakage current was negligible (less than 1 nA) below 100 °C but increased substantially with temperature to the microampere level at 230 °C and reached 40 μA at 370 °C, a level significantly larger than the electrochemical signals (~nA) produced at this Pt electrode. Thus, useful electrochemical measurements were not possible with Pyrex insulated UMEs at temperatures above 230 °C. The ionic conductivity of Pyrex glass is known to increase with temperature.<sup>16,17</sup> Although this increase is tolerable with conventional (millimeter-sized) electrodes, it is unsatisfactory for UMEs.

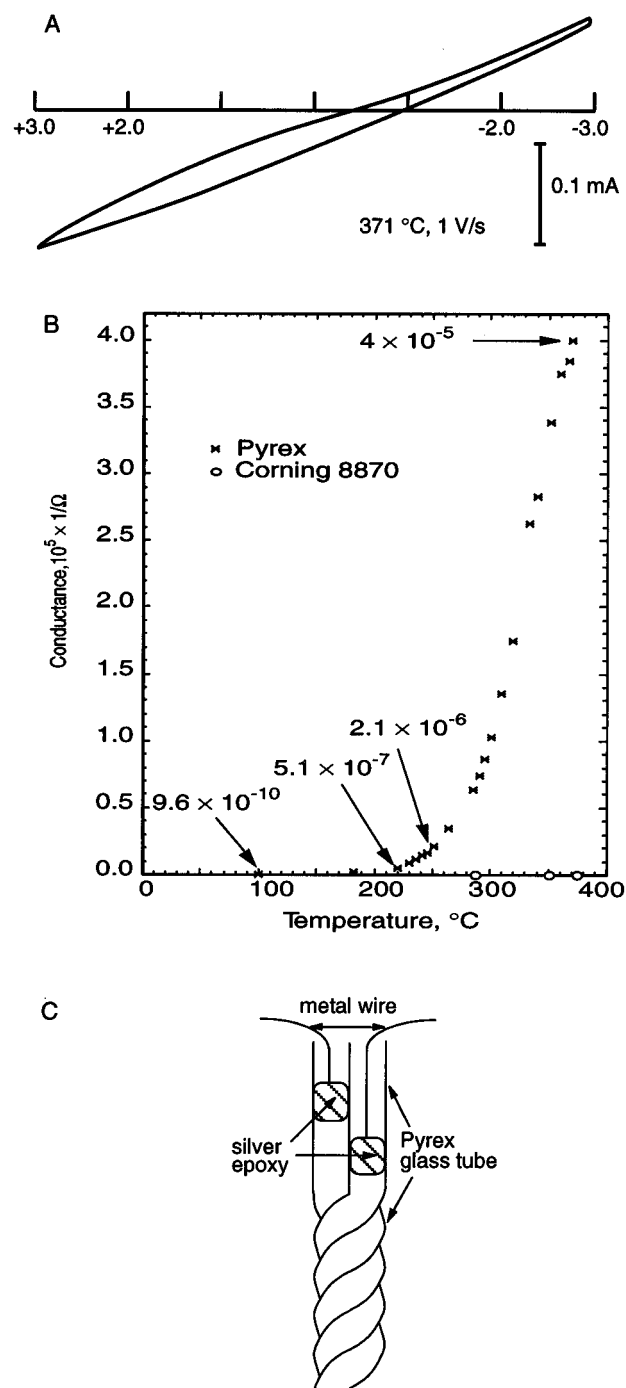


**Figure 2.** (A) *i*-*V* curve of Pyrex glass in water at a pressure of 240 bar without exposing the Pt electrode to water, i.e., the current conducted through the glass. (B) Conductance of Pyrex and Corning 8870 glass as a function of temperature. Scan rate, 100 mV/s. (C) Schematic diagram of the Pyrex glass electrode used in the *i*-*V* measurements to confirm the glass conductivity.

To demonstrate that the observed current leakage was not caused by cracks in the glass, leakage at high temperatures of water between the glass and Pt wire, or water interaction with the glass, an experiment was carried out with two Pt wires sealed separately in glass in the absence of any water phase. Two drawn glass capillaries were intertwined by heating and twisting in a flame. Then a Pt wire was introduced into the larger open end of each capillary and affixed to the wall with silver epoxy cement, as shown in Figure 2C. This was placed in an oven, and the *i*-*V* behavior (current flow between the electrode as a function of applied potential) was investigated as a function of temperature. In this experiment, the only possible current path

between the two electrodes under bias was through the glass walls. The  $i$ - $V$  curves obtained were comparable to those obtained with the electrochemical cell (Figure 2A), indicating that the leakage current was caused solely by the conductivity increase in Pyrex glass with temperature.

The  $i$ - $V$  curves obtained in solutions at higher temperatures were independent of scan rate. For example, even at a relatively low temperature of 260 °C, the  $i$ - $V$  curve was essentially a straight line with little evidence of hysteresis within a potential range of -3.2 to +3.2 V at scan rates over 4 orders of magnitude (5 mV/s to 10 V/s). Thus, it was not possible to eliminate leakage currents by using smaller scan rates in the CV measurements. The glass conductivity increase with an onset at  $\sim$ 230 °C coincides with the temperature beyond which CVs obtained with Pyrex glass-sealed electrodes show significantly distorted shapes. Thus, good CVs cannot be obtained with Pyrex glass-based UMEs at higher temperatures. Fused quartz was also not useful because of the large mismatch of its thermal expansion coefficient ( $0.55 \times 10^{-6}/^{\circ}\text{C}$ ) compared to Pt wire ( $9.1 \times 10^{-6}/^{\circ}\text{C}$ ) as well as the severe corrosion observed with this material. Several quartz-based electrodes were tried but showed no improvement over the Pyrex-based electrodes. What is required is a glass that shows low conductivity at high temperatures, a good match to the thermal expansion coefficient of Pt, and a reasonable resistance to corrosion in high-temperature water. These criteria were met by Corning 8870 glass, which has a composition of 25–35% silica, 50–60% lead oxide, 5–10% potassium carbonate, 1–5% potassium nitrate, and 0.1–0.5% antimony oxide, a thermal expansion coefficient of  $9.1 \times 10^{-6}/^{\circ}\text{C}$ , and an electrical resistivity as high as  $10^{9.5}$  ohm cm at 350 °C. Moreover, no evidence of corrosion was detected on the glass surface after working under supercritical conditions (385 °C) in 0.2 M NaHSO<sub>4</sub>. Thus, although it is expensive and difficult to work with in electrode fabrication, Corning 8870 was used for all studies reported below. Two electroactive species, iodide and hydroquinone, were chosen to evaluate UMEs made with this glass and to explore the possibility of electrochemical studies in supercritical water at an UME.

**Voltammetry of KI.** The CV behavior of I<sup>-</sup> in initially 0.2 M NaHSO<sub>4</sub> was studied up to 385 °C (Figure 3). At 23 °C, I<sup>-</sup> was oxidized to I<sub>2</sub> in a forward scan toward positive potentials. Note that the electrogenerated iodine was not soluble at this concentration of I<sup>-</sup> and precipitated on the Pt electrode surface. The I<sub>2</sub> deposit was stripped off in the reverse potential scan and appears as a cathodic peak (Figure 3A). This precipitation does not persist at higher temperatures where the solubility of iodine is higher. A well-defined CV curve with little or no hysteresis on scan reversal was obtained at higher temperatures (Figure 3B). The sigmoidal shape, rather than a peak-shape, is characteristic in CVs at UMEs where nonlinear (hemispherical) diffusion prevails.<sup>14</sup> The well-defined shape and reproducibility of these CVs demonstrate that an excellent seal could be achieved with the Corning 8870 glass. The steady-state current increased strongly with temperature because of the increase in diffusion rates. Well-behaved CVs were obtained at 250 °C (Figure 3C) and above; this had not been possible in the previous studies with Pyrex glass-based UMEs. An even more dramatic improvement was seen at 301 °C and above (curves D and E of Figure 3), demonstrating that Corning 8870 glass was quite suitable for high-temperature electrochemical studies. Note that the concentration of I<sup>-</sup> in solution decreased because of solution expansion with temperature. The effect of decreased concentration on the limiting current was offset, however, by the large increase in the diffusion coefficient of the electroactive species. Moreover, large changes occur with temperature at constant

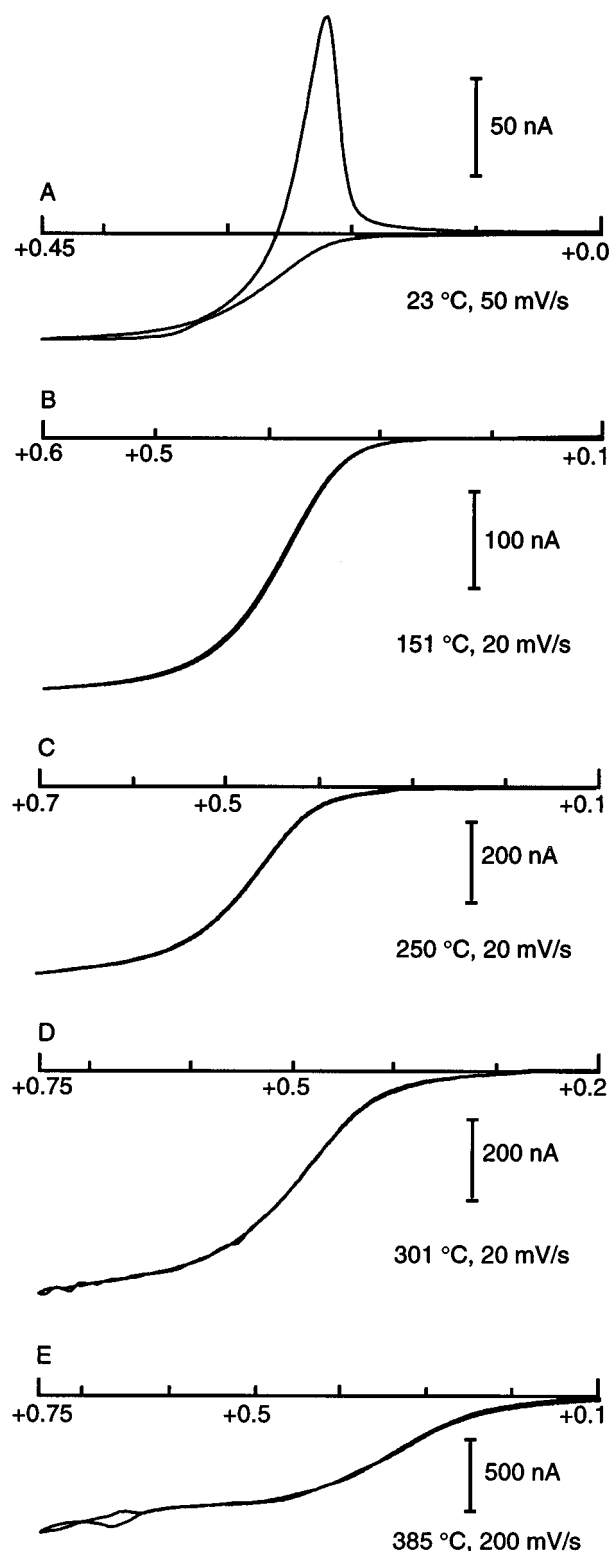


**Figure 3.** Representative cyclic voltammograms of 5.8 mM KI in 0.2 M NaHSO<sub>4</sub> at a Pt UME ( $r = 14.5 \mu\text{m}$ ) at different temperatures. Pressure was 150 bar for A–D and 270 bar for E.

pressure in certain regions. For example, at a pressure of 200 bar, the specific volume of water increases 3.5 times when temperature only increases from 365 to 370 °C. This gives rise to the large changes in the current magnitude observed experimentally. At a given temperature, variation of pressure has a similar effect.<sup>11</sup> Therefore, good control of the temperature and pressure is needed near these points to obtain stable CVs. The current became very sensitive to the stability of temperature and pressure under supercritical conditions. This is one source

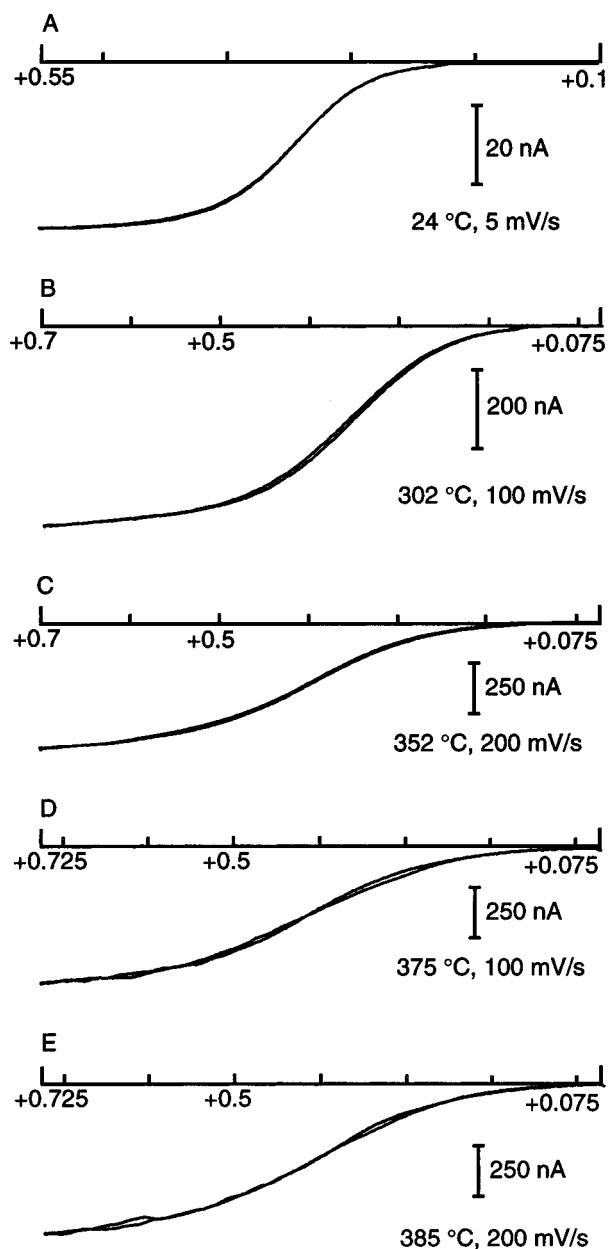


**Figure 4.** Cyclic voltammograms of 5 mM hydroquinone in 0.2 M NaHSO<sub>4</sub> at a Pt UME ( $r = 14.5 \mu\text{m}$ ) at different temperatures. Pressure was 175 bar for curves A and B, 225 bar for curve C, 240 bar for curve D, and 270 bar for curve E.

of the greater variations seen in the CVs at higher temperatures (Figure 3E).

**Voltammetry of Hydroquinone.** The high solubility of hydroquinone in aqueous solution at room temperature and its stability in supercritical water made it possible to study this organic species over the entire temperature range of interest. The CVs obtained in initially 0.2 M NaHSO<sub>4</sub> at different temperatures and pressures are shown in Figure 4. The CVs were obtained in sequence with increasing temperature (from A to E), and they reproduced as well when the temperature was decreased. At room temperature, for example, the CVs measured at the same electrode before and after the studies in supercritical water were essentially identical. This is consistent with the fact that the electrode appeared the same under an optical microscope before and after the experiments, with no erosion of the Pt surface or the surrounding glass sheath for experiment durations of at least 3 h. The good quality CVs obtained at both ambient and high temperatures again demonstrate the excellent seal provided by the Corning 8870 glass

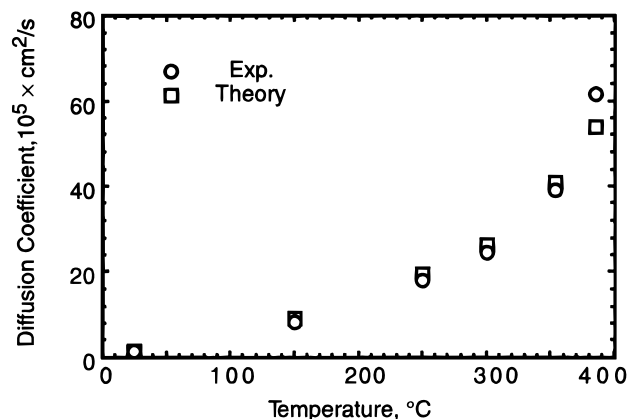


**Figure 5.** Diffusion coefficient of iodide ions as a function of temperature in water.

and suggest that it will be possible to study a wide variety of species under near-critical and supercritical conditions at a UME. The CVs in Figure 4 also show that the hydroquinone/benzoquinone redox couple is quite stable in supercritical water in the absence of oxygen and that it can be studied with a simple electrochemical technique. Electrochemical techniques provide a direct in situ probe capable of investigating a variety of physical and chemical properties, including the thermodynamics and kinetics of many reactions of organic compounds. The increased solubility of organic compounds in high-temperature water may also be useful in the design of new electroorganic syntheses.<sup>10,12</sup>

**Diffusion Coefficients.** The well-defined plateau in the CVs shown in Figures 3 and 4 represents the control by hemispherical diffusion of the electroactive species toward the Pt disk electrode. This allows the calculation of the diffusion coefficient for I<sup>-</sup> and hydroquinone from the limiting current from the equation<sup>14</sup>

$$i_l = 4nFrDc \quad (1)$$

where  $i_l$  is the limiting current,  $n$  is the number of electrons transferred,  $F$  is the Faraday constant,  $r$  is the radius of the electrode,  $D$  is the diffusion coefficient, and  $c$  is the concentration of the electroactive species. To apply this equation to studies at high temperature, correction must be made to account for the expansion of the solution, which causes a drop in the concentration of the diffusing species. The reduction in the density of water as a function of temperature and pressure was obtained from the ASME Steam Tables,<sup>18</sup> assuming the density of 0.2 M NaHSO<sub>4</sub> followed that of pure water.

The measured diffusivities for iodide and hydroquinone were compared with the values theoretically predicted by the Stokes–Einstein relation<sup>19</sup>

$$D = kT/(6\pi\eta a) \quad (2)$$

where  $k$  is Boltzmann's constant,  $T$  is temperature,  $\eta$  is the solution viscosity, and  $a$  is the effective radius of the diffusing species. Deviations from this relation at higher temperatures would indicate changes in the nature of the electroactive species, e.g., in the radius of the hydrated ions. Figures 5 and 6 are a comparison of the experimental diffusion coefficients with those calculated from eq 2 as a function of temperature and pressure. The agreement between the experimental and theoretical data is very good for both iodide and hydroquinone. This agreement suggests that there are no large changes in the size or shape of these diffusing species and that the changes in water for

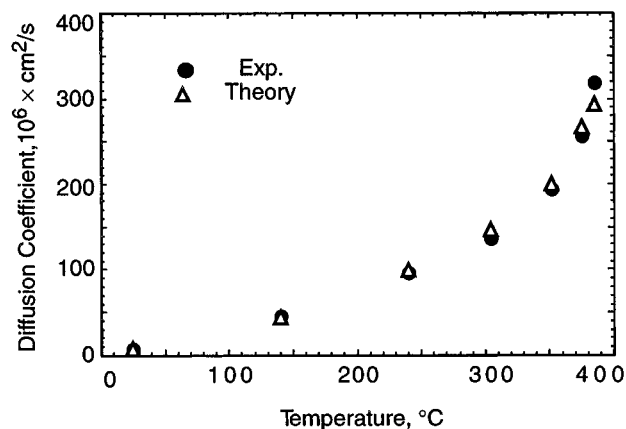


**Figure 6.** Diffusion coefficient of hydroquinone as a function of temperature in water.

**TABLE 1: Experimental and Theoretical Diffusion Coefficients of Iodide Ions at Different Temperatures and Pressures**

T, °C	P, bar	density <sup>a</sup>	D, 10 <sup>5</sup> cm <sup>2</sup> /s	
			experiment <sup>b</sup>	theory <sup>c</sup>
25	150	1.004	1.47	1.37
150	150	0.925	8.32	9.27
250	150	0.811	18.21	19.57
300	150	0.726	24.58	26.41
354	200	0.582	39.12	40.99
385	270	0.448	61.74	53.79

<sup>a</sup> From ref 18, at 25 °C and 1 bar = 1.000. <sup>b</sup> *c* = 5.8 mM, *r* = 14.5 μm. <sup>c</sup> Calculated from Stokes–Einstein equation with *a* = 1.8 Å.

**TABLE 2: Experimental and Theoretical Diffusion Coefficients and  $E_{3/4} - E_{1/4}$  of Hydroquinone at Different Temperatures and Pressures**

T, °C	P, bar	density <sup>a</sup>	D, 10 <sup>6</sup> cm <sup>2</sup> /s		$E_{3/4} - E_{1/4}$ <sup>d</sup>	
			expt <sup>b</sup>	theory <sup>c</sup>	expt <sup>e</sup>	calcd <sup>f</sup>
25	175	1.005	7.55	7.46	69	28.2
140	175	0.935	45.56	44.43	92.5	39.1
240	175	0.828	96.01	98.96	106	48.6
304	175	0.722	135.87	146.24	127	54.6
352	225	0.607	193.87	200.45	147	59.2
375	240	0.485	256.91	266.84	162	61.4
385	270	0.449	317.16	293.45	167.7	62.3

<sup>a</sup> From ref 18, at 25 °C and 1 bar = 1.000. <sup>b</sup> *c* = 5 mM, *r* = 14 μm. <sup>c</sup> Calculated from Stokes–Einstein equation with *a* = 3.3 Å. <sup>d</sup> The potentials  $E_{3/4}$  and  $E_{1/4}$  are those for which  $i = 3i/4$  and  $i = i/4$ , respectively. <sup>e</sup> Raw data without correction or *iR* compensation. <sup>f</sup> Calculated from Tomes' criterion<sup>20</sup> for an ideal reversible couple with *n* = 2.

diffusion can be largely treated in terms of bulk viscosity changes. The advantage of using a UME in this supercritical water study can be contrasted to the previously reported results using macroscopic Pt electrodes,<sup>10</sup> where significant positive deviations of the experimental diffusivity from the theoretical prediction were observed. Moreover, the diffusion coefficient of hydroquinone could not be obtained above 300 °C, even at a rather small electrode ( $\sim 1.9 \times 10^{-3}$  cm<sup>2</sup>) by chronoamperometry.<sup>10</sup>

The reduced ohmic potential drop found with UME measurements should allow better measurements of thermodynamic (half-wave) potentials and heterogeneous electron-transfer kinetics. According to Tomes' criterion of reversibility,<sup>20</sup> at 25 °C  $E_{3/4} - E_{1/4} = 28.2$  mV for a thermodynamically reversible couple with *n* = 2 (here,  $E_{3/4}$  and  $E_{1/4}$  are the potentials for  $i = 3i/4$  and  $i = i/4$ , respectively). For hydroquinone,  $E_{3/4} - E_{1/4} = 69$  mV at room temperature, suggesting a nonreversible

oxidation process probably because of involvement of deprotonation steps in the electron transfer. This can also be seen in the slow rising current onset in Figure 4. Moreover, the potential difference calculated from the raw data increases with temperature and pressure, as shown in Table 2. In general, *iR* drop and kinetics are primarily responsible for sluggish behavior. Here, *iR* drop was estimated from published conductance data of 0.1 M NaCl in aqueous solution<sup>21</sup> up to about 300 °C at temperatures and densities of water close to those under which our CVs were obtained. Over the temperature range 25–304 °C, the ionic mobilities and hence the conductance increase rapidly with increasing temperature because of the sharp decrease in the viscosity and dielectric constant. The calculated *iR* drop at 304 °C is less than 1 mV and is too small to account for the increase of irreversibility of hydroquinone oxidation as indicated by  $E_{3/4} - E_{1/4}$ . Kinetic contributions must dominate at the high temperatures. Although a temperature increase alone should enhance the kinetics for most chemical reactions, changes in solvent properties, such as dielectric constant and density of water, which can strongly affect solvation at high temperature, must also be considered. More detailed studies of electrochemical kinetics in water at high temperature are under way.

**Acknowledgment.** We are indebted to Dr. F.-R. F. Fan for valuable discussions. The support of this research by a URI grant from the Army Research Office is gratefully acknowledged.

## References and Notes

- (1) Franck, E. U. *J. Solution Chem.* **1973**, *2*, 339.
- (2) Franck, E. U. In *High-Pressure Chemistry*, Proceedings of the NATO Advanced Study Institute, Corfu, Greece, September 24–October 8, 1977; Kelm, H., Ed.; NATO Advanced Study Institute Series C, 41; D. Reidel: Dordrecht, Holland, 1978; p 221.
- (3) Marshall, W. L.; Franck, E. U. *J. Phys. Chem. Ref. Data* **1981**, *10*, 295.
- (4) Todheide, K. In *Water: A Comprehensive Treatise*; Franks, F., Ed.; Plenum Press: New York, 1972; Vol. 1.
- (5) Osugi, J.; Shimizu, K.; Nakahara, M.; Hirayama, E.; Matsubara, Y.; Ueno, M. In *Proceedings of the 4th International Conference on High Pressure in Semiconductor Physics*; Journal of Applied Physics: Kyoto, 1975; p 610.
- (6) Marshall, W. L. In *High Temperature High Pressure Electrochemistry in Aqueous Solutions*; National Association of Corrosion Engineers: Houston, TX, 1976; Vol. NACE-4, p 117.
- (7) (a) Thomason, T. B.; Modell, M. *Hazard. Waste* **1984**, *1*, 453. (b) Modell, M. U.S. Patent 4 338 199, 1982.
- (8) Macdonald, D. D. In *Modern Aspects of Electrochemistry*; Conway, B. E., Bockris, J. O'M., Eds.; Plenum: New York, 1975; Vol. 11, p 141.
- (9) McDonald, A. C.; Fan, F.-R. F.; Bard, A. J. *J. Phys. Chem.* **1986**, *90*, 196.
- (10) Flarsheim, W. M.; Tsou, Y.; Trachtenberg, I.; Johnston, K. P.; Bard, A. J. *J. Phys. Chem.* **1986**, *90*, 3857.
- (11) Flarsheim, W. M.; Bard, A. J.; Johnston, K. P. *J. Phys. Chem.* **1989**, *93*, 4234.
- (12) Bard, A. J.; Flarsheim, W. M.; Johnston, K. P. *J. Electrochem. Soc.* **1988**, *135*, 1939.
- (13) Gaul, E. *J. Chem. Educ.* **1993**, *70*, 176.
- (14) Wightman, R. M.; Wipf, D. O. In *Electroanalytical Chemistry*; Bard, A. J., Ed; Marcel Dekker: New York, 1989; Vol. 15, p 267.
- (15) Wehmeyer, K.; Wightman, R. M. *J. Electroanal. Chem.* **1985**, *196*, 417.
- (16) Morey, G. W. *The Properties of Glass*, 2nd ed.; Reinhold Publishing: New York, 1954.
- (17) Kriksunov, L. B.; Macdonald, D. D. *Sens. Actuators* **1994**, *B22*, 201.
- (18) Haar, L.; Gallagher, J. S.; Kell, G. S. *NBS/NRC Steam Tables*; Hemisphere Publishing: Washington, DC, 1984.
- (19) Bird, R. B.; Stewart, W. E.; Lightfoot, E. N. *Transport Phenomena*; Wiley: New York, 1960; Chapter 16.
- (20) Tomes, J. *Collect. Czech. Chem. Commun.* **1937**, *9*, 12, 81, 150.
- (21) Quist, A. S.; Marshall, W. L. *J. Phys. Chem.* **1968**, *72*, 684.